A Statistical Model for Signal-Dependent Charge Sharing in Image Sensors

Konstantin D. Stefanov

***Abstract*—A Monte Carlo model based on signal-dependent charge sharing mechanism during charge collection has been developed to explain the non-linearity of the Photon Transfer Curve (PTC) in image sensors. The model is based on tracing of individual electrons generated by Poisson-distributed photons and describes the PTC non-linearity as a process with sub-Poisson variance, with excellent qualitative agreement with the experimental data. A new PTC curve fitting formula is proposed, taking into account this non-linearity. The new formula is an excellent fit to the data, does not require selection of linear section of data points and allows more robust calculation of the system conversion gain.**

***Index Terms*—Photon Transfer Curve, Sub-Poisson Noise**

I. Introduction

THE Photon Transfer Curve (PTC) [1] is an extremely useful method for obtaining the conversion gain of photon imaging systems, and is used extensively for characterization and parameter optimization of Charge Coupled Devices (CCDs) and Complementary Metal-Oxide-Semiconductor (CMOS) image sensors. Accurate determination of the conversion gain, usually expressed as electrons per Analog-to-Digital conversion Unit (e-/ADU), allows system calibration in fundamental units – the number of collected photoelectrons. The conversion gain is the basis for the calculation of many important imager parameters such as quantum efficiency, dark current, noise and full well capacity.

The PTC method relies on Poisson statistics for obtaining valid results and is underpinned by the concept that the light stimulus consists of random, Poisson-distributed photons. If each interacting photon generates a photoelectron, which is then collected in a statistically independent way, the signal (i.e. the number of collected photoelectrons during the integration time) is also Poisson-distributed, giving rise to shot noise. When expressed in electrons, the plot of the signal variance versus the mean signal has a slope of unity, as dictated by Poisson statistics. The system conversion gain K is obtained as the inverse of the slope of the shot noise dominated signal variance σ_{shot}^2 versus the mean signal S, when both are expressed in ADU [1]:

$$\sigma_{shot}^{\ 2}(ADU) = \frac{S(ADU)}{K(e-/ADU)}. \quad (1)$$

Under constant illumination, the collected photo-generated signal is a linear function of the exposure time, provided that sensor's response is linear too. This is usually the case for CCDs, but a modified PTC method can successfully be used even for imagers with significant gain non-linearity to calculate the quantum efficiency [2].

Previous studies on CCDs [3][4] have found significant (in excess of 15%) non-linearity of the PTC and sub-Poisson signal variance despite the fact that the photo response is linear to much better than 1%. An example PTC is shown in Fig. 1 and the corresponding photo response over the same signal range is shown in Fig. 2. The signal variance reaches a peak at mean signal around 3500 ADU and then decreases due to the onset of pixel saturation which limits the signal statistics, and is a well understood effect. However, the variance is significantly non-linear at much lower signal levels *before* well saturation is reached, and this is the subject of the present paper.

The PTC non-linearity is potentially a source of error in the calculation of the conversion gain because the method relies on a linear PTC obeying Poisson statistics. A detailed investigation [3] has excluded a large number of possible mechanisms for generating this effect and has concluded that a form of charge sharing between pixels is the most likely cause. Still, there is no available model capable of explaining the observed non-linear variance.

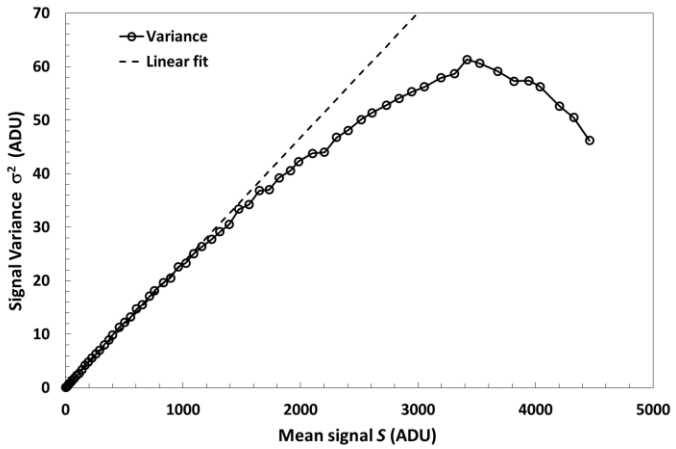

Fig. 1. Photon transfer curve of CCD204 obtained with light with wavelength of 660 nm.

Manuscript received June 27, 2013.
Konstantin D. Stefanov is with the e2v Centre for Electronic Imaging, The Open University, Walton Hall, Milton Keynes, MK7 6AA, UK (e-mail: Konstantin.Stefanov@open.ac.uk).

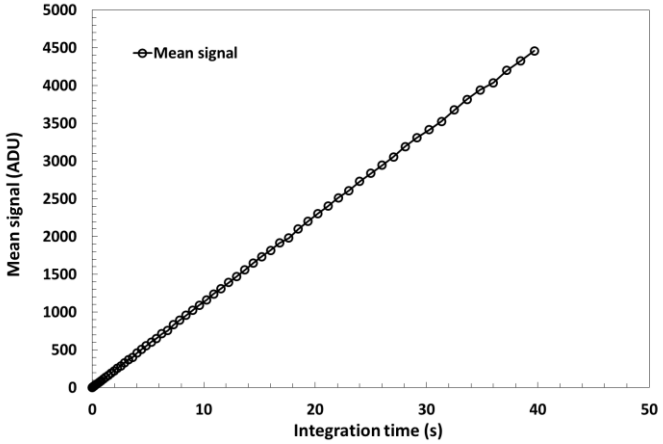

Fig. 2. Photo response of CCD204 obtained with light with wavelength of 660 nm. The linearity is better than ±1%.

Sub-Poisson signal statistics arising in charge collection in back-illuminated CCD has been observed previously [5], and has been attributed to non-linear charge collection efficiency caused by an electronic shutter structure. In the work by R. Reich this is caused by the formation of potential barrier with increasing height, depending on the amount of collected charge. This creates non-linear signal variance similar to the observations in CCDs, but as will be shown further the underlying mechanism is very different.

Over the last few years a number of projects at the e2v Centre for Electronic Imaging on advanced CCDs for space telescopes like Gaia and Euclid have accumulated large sets of CCD data, which helped in formulating the ideas presented in this paper. Here we present a new model based on signal-dependent charge sharing, simulate its properties using Monte Carlo (MC) method and apply the results to experimental CCD data showing non-linear PTC.

II. Charge Sharing Model

A. Rationale

One important clue emerging from previous investigations on back-illuminated CCDs with thick substrates [4] is that the PTC non-linearity tends to increase with the thickness of the photosensitive silicon, suggesting that some effect occurring *during* charge collection is responsible. Once the charge has been collected, sharing between stored signals becomes unlikely due to the large potential barrier between the signal packets. Spatial autocorrelation analysis supports the charge sharing hypothesis [3] but does not provide further insights. The same work excludes lateral diffusion of charge in field-free regions, charge sharing during transfer in both serial and parallel registers, the output amplifier and the electronics as possible sources of the effect. Charge sharing in fully depleted CCDs caused by lateral diffusion is well understood [6], however the standard macroscopic treatment using drift and diffusion equations cannot address the statistics of charge collection.

Our model is inspired by the experimental method used for obtaining the photo response of CCDs using flat field illumination; this method is used for plotting the PTC and for calculating the linearity of the device. The PTC is obtained by taking series of two flat field images at the same light intensity and subtracting them to eliminate the fixed pattern noise caused by pixel non-uniformity. The light intensity spans from zero to a level where the full well capacity is exceeded. The signal variance is calculated from the variance of the resulting difference image divided by two, after subtracting the system readout noise, which leaves only the shot noise.

Considering the non-linear PTC in flat field illumination conditions has the important advantage that each pixel has the same mean signal even if the variance deviates from the Poisson distribution. Any model attempting to explain the PTC non-linearity has to be able to generate the same uniform mean response.

Further in the paper CCD description and terminology is used, however the discussions are applicable to CMOS or other image sensors where similar charge collection takes place. Modern CCDs exhibit very small signal non-linearity, usually dominated by the charge-to-voltage conversion at the output node and the source follower, and this allows the effects of PTC and output non-linearity to be easily discriminated. For this reason all the experimental data presented here were obtained with a state of the art CCD intended for scientific applications.

B. Model Description

1) Mechanism

A series of diagrams illustrating the concept of signal-dependent charge sharing are shown in Fig. 3. The diagrams study three pixels in one dimension, however similar considerations are also applicable to two dimensions. By applying boundary conditions that make Pixel 1 and Pixel 3 neighbors, the model can be made to represent infinite number of 1-D pixels.

Under idealized conditions with no charge sharing (Fig. 3(a)), each electron is collected in the pixel volume it was generated. Since the rate of photoelectron generation is governed by the rate of incoming photons, the number of collected electrons will follow Poisson statistics. During signal integration the number of collected electrons in each well increases at a mean rate proportional to the light intensity, but with statistical fluctuations. At any point of time during collection the number of stored electrons in the three pixels will in general be different and will deviate from the mean for that time. As the potential wells get filled up, the peak well potential and the electric field in the depletion layer will decrease [7], affecting the charge collection process. However, if charge sharing does not take place the electron collection rate will be *unaffected* as it is determined by the photon arrival rate, and the signal variance will equal the signal mean.

The experimental data strongly suggests that there is charge sharing during collection and that it does not affect the mean collected signal under flat field illumination conditions. However, if the sharing is random (i.e. the sharing factor is constant) the signal would still be Poisson-distributed. As

stated in the Burgess variance theorem, random selection of events from a Poisson process is still a Poisson process.

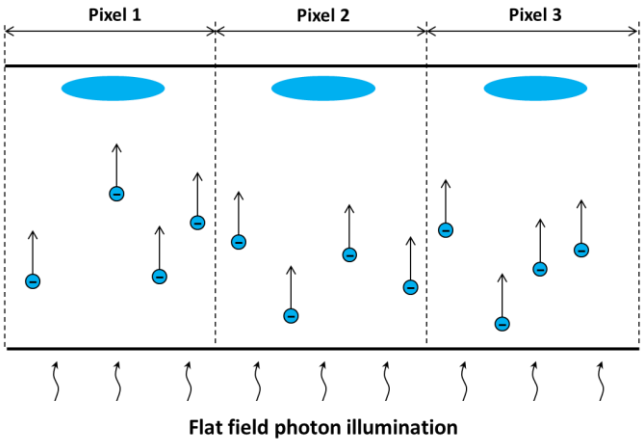

Fig. 3(a). Idealized charge generation and collection without charge sharing in a fully depleted device.

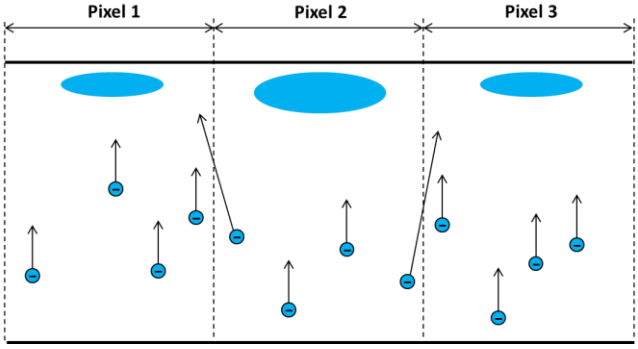

Fig. 3(b). Charge sharing prompted by the larger number of stored electrons in the potential well of Pixel 2.

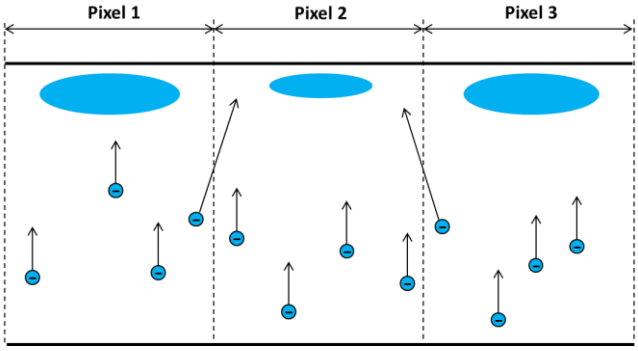

Fig. 3(c). Charge sharing prompted by the fewer number of stored electrons in the potential well of Pixel 2.

To explain the observed sub-Poisson variance the proposed model suggests that there is a correlation mechanism in the electron collection process, and that the mechanism is realized through a charge sharing probability, which is a function of the already collected charge. The suggestion is that charge sharing increases when there is a difference between the numbers of collected electrons in adjacent pixels.

Fig. 3(b) shows a moment of time when the number of collected photoelectrons in Pixel 2 is larger than in the neighbor pixels. At that time the well potentials of Pixel 1 and Pixel 3 will be slightly higher than Pixel 2 and therefore more attractive to photoelectrons generated in the volume of Pixel 2. Through the proposed mechanism there will be a small probability that a photoelectron generated in Pixel 2 will end up either in Pixel 1 or Pixel 3.

The probability of charge sharing P_i, defined as the probability of *not collecting* a photoelectron generated in the volume of pixel i in the potential well of the same pixel is expressed as

$$P_i = \left(\frac{\alpha}{FW}\right)\left(n_i - \frac{1}{3}\sum_{j=1}^{3} n_j\right), \tag{2}$$

where α is an empirical dimensionless sharing coefficient, FW is the full well capacity in electrons and n_i is the present number of electrons in pixel i. The equation describes signal-dependent charge sharing with probability proportional to the difference between the instantaneous number of electrons n_i in a pixel and the average number of electrons over all pixels.

In (2) the number of electrons is used as a proxy for the electric field experienced by the collected charge, which in fact controls charge behavior. In principle, the electric field in the device can be expressed as a function of the number of electrons stored in each potential well. Detailed field calculation is device specific and likely to be treatable only by finite element analysis due to its complexity. The equation (2) can be considered as an approximate, leading order macroscopic description of the mechanisms leading to non-zero probability of charge sharing.

Fig. 3(c) shows a moment of time when the number of collected photoelectrons in Pixel 2 is smaller than in the neighbor pixels, making it more attractive for incoming electrons. Using (2) the sharing probability for each pixel can be calculated, and for the diagram on Fig. 3(c) we can deduce that $P_1, P_3 > 0$ and $P_2 < 0$.

P_i gives the probability of an electron being attracted to one of the neighbor pixels. When $P_i < 0$ the probability of sharing is taken to be zero, and the electron is collected in the pixel where it was generated. The electrons traversing near the edge of a pixel boundary are the most likely ones to experience charge sharing and be collected in the corresponding neighbor pixel. In a simple model (Lowest Neighbor, or LN) the neighbor with the lowest number of electrons will receive the shared electron. This model ignores the spatial distribution of the incoming photoelectrons, but still can be a useful approximation of the physical process. The LN model has two sources of charge collection correlation – one from the difference between the signal in pixel i and the mean, and another from the allocation of charge to the lowest neighbor.

Even simpler would be to assign the collecting pixel at random (Random Neighbor, or RN), although this obviously deviates more from the real process of charge sharing and reduces the level or correlation. In the following section the LN model is simulated using MC method.

The described algorithm can be modeled as a Markov chain

where each state is described by the number of stored electrons in the potential wells. In a Markov chain the probability of obtaining the next state depends only on the present state and the process has no memory, as in the described charge sharing model. In principle, the variance of such Markov process can be calculated, but the use of Monte Carlo methods is far more practical.

2) Signal Variance

The effect of the signal-dependent charge sharing on the signal variance can be explained by the introduced correlation in the charge collection process. The collection rate for a pixel increases when the stored charge is less than the average and decreases when it is more than the average, with the charge sharing mechanism acting in a way similar to negative feedback. The charge collection rate therefore becomes more equalized, or less random. Since the signal is the number of collected photoelectrons over time, it is apparent that the statistical fluctuations of the signal will be lower than the incoming Poisson-distributed photons.

The charge already collected in the potential wells affects where the next photoelectrons will be collected, thus introducing correlations between the signal carriers. The outcome can be thought of as a form of Fano factor, however there are two significant differences. Unlike the Fano factor, which is caused by correlations in the process of *charge generation*, the mechanism described here causes sub-Poisson signal variance during *charge collection*. The other significant difference, to be demonstrated in the following section, is that the signal variance is a non-linear function of the signal, and therefore distinct from the Fano mechanism.

3) Characteristics

Based on the described mechanism we can predict some of the expected characteristics of the model. Firstly, since the incoming photoelectrons are influenced by the electric field in the volume of the device (which changes due to the stored charge), we can conclude that electrons diffusing in field-free regions will be unaffected. The signal variance of shared charge through diffusion is expected to be Poisson-distributed, the same as the incoming photons.

The sharing coefficient α is introduced to account for the probability of charge sharing and the ratio α/FW can be considered to be a normalizing factor to ensure that the probability is not greater than 1. In CCDs the depleted and field-free regions do not change significantly in size as the signal is collected to full well due to the relatively small change of the channel potential, therefore for photoelectrons generated *outside* the depleted region the coefficient α should be constant. As the wavelength of the illumination increases more photoelectrons will be generated *inside* the depleted region and closer to the potential wells. This will reduce the probability of interaction and some decrease of α with increasing wavelength is expected. The coefficient α is expected to increase with the size of the depleted region due to the longer electron path and the increased probability of interaction, as backed by previous investigations [4].

For the RN model with constant sharing probability P_i the charge will be allocated to the potential wells at random, and its variance will be equal to the mean. For the LN model this is not true because the simulated charge collection to the pixel with the lowest number of stored electrons introduces a separate correlation leading to sub-Poisson variance. These characteristics can be used to verify the validity of the numerical model by setting $P_i = const$.

C. Monte Carlo Model

The model described above was implemented in a MC algorithm written in MATLAB. The code was written for 3 pixels, and the boundary conditions were such that the right side neighbor of Pixel 3 is Pixel 1, and similarly the left side neighbor of Pixel 1 is Pixel 3. The algorithm tracing one photoelectron consists of the following steps:

- Simulate an electron from a Poisson process with mean 3λ;
- Randomly assign the electron to pixel *i*=1, 2 or 3 (this creates an independent Poisson process for each pixel);
- Calculate the sharing probability using (2);
- If $P_i \leq 0$ collect the electron to pixel *i*;
- If $P_i > 0$ generate a random number *R* in the range (0, 1);
- Lowest Neighbor Model: if $P_i > R$ collect to the neighbor pixel with the lowest number of stored electrons; else collect to pixel *i*
  Random Neighbor Model: if $P_i > R$ collect to a neighbor pixel at random; else collect to pixel *i*.

This MC algorithm simulates collected photoelectrons in each pixel with mean λ. The calculated mean is λ regardless of the value of α, as required from the conditions of flat field illumination. The variance is calculated after running the algorithm a large number of times to reduce the statistical error to a negligible level. It was also verified that when P_i is constant the RN model generates Poisson-distributed electron numbers with variance equal to the mean, as expected.

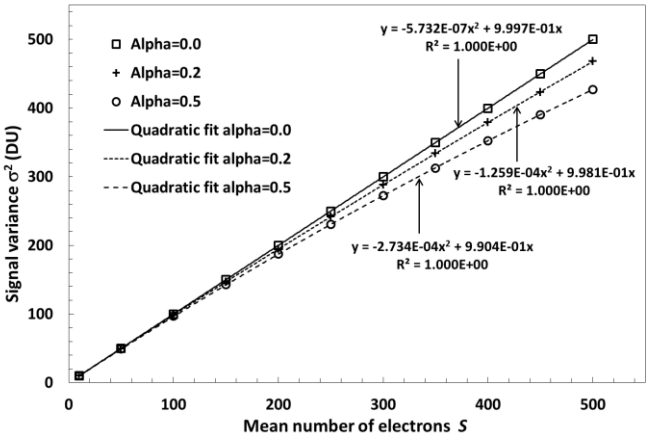

Fig. 4. MC simulation of the variance versus mean in dimensionless units (number of electrons) for different α and *FW*=1000, with quadratic fit to the data points.

The generated mean-variance plots for the LN model with three different values of the parameter α and *FW*=1000 e- are

shown in Fig. 4. The plots for $\alpha > 0$ are clearly non-linear, and it was found that the quadratic function

$$\sigma_{shot}^2 = \gamma S - \nu S^2 \quad (3)$$

is an excellent fit to the simulated data. In (3) S is the mean number of photoelectrons, γ is a gain factor and ν is a non-linearity parameter. The same data is plotted in Fig. 5 as the difference between mean and variance so that the non-linearity can be better appreciated. The mean to variance ratio is shown in Fig. 6, demonstrating linear increase with the signal size.

The RN model produces very similar results, however the signal correlation is smaller and correspondingly the non-linearity of the variance is lower than the LN model.

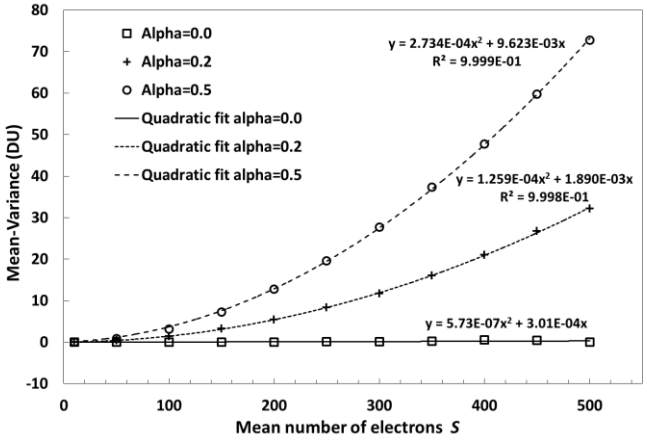

Fig. 5. Difference between mean and variance for the data in Fig. 2, with quadratic fit to the data points.

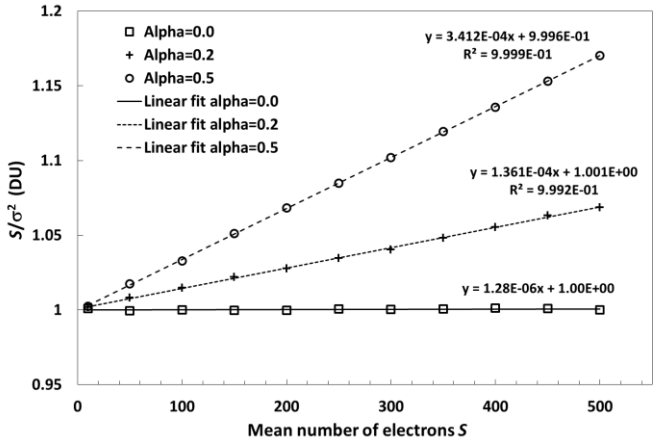

Fig. 6. Ratio of the mean signal to its variance as a function of the mean signal.

The gain γ is very close to unity as expected from the Poisson distribution. For $\alpha = 0$ the variance is linear and $\nu = 0$, $\gamma = 1$ as expected; however the simulated data for $\alpha = 0$ were fitted with a quadratic function as for $\alpha > 0$. This is used to verify the quality of the quadratic fit and the MC algorithm when ν is expected to be zero. The fit in Fig. 4 gives three orders of magnitude lower value for ν when charge sharing is not present ($\alpha = 0$).

The second term in (3) can be considered as a second-order correction to the PTC equation. In the absence of signal-dependent charge sharing ν is zero and (3) becomes the "classic" PTC relationship (1) where $\gamma = 1/K$. Therefore, the first term in (3) can be used for calculation of the system conversion gain. The non-linear term ν does not affect the gain calculation.

III. Experimental Data

The predictions from the MC model were compared to experimental data obtained with back illuminated (BI) CCD. The illumination was generated by LEDs at three wavelengths – 850 nm, 660 nm and 470 nm. The signal mean and variance were obtained using the procedure described in Section II. The device under test was e2v CCD204, a 4-phase BI deep depletion type CCD with 40 µm thick epitaxial layer and 130 ke- full well capacity.

A. Signal Linearity

The plot of the signal mean as a function of the integration time for 660 nm illumination is shown in Fig. 2. The residuals from the linear fit show signal linearity better than ±1% up to integration time of 30 seconds, corresponding to approximately 120 ke- stored charge. As the integration time is increased further the full well capacity of the device is exceeded and the response starts to deviate significantly from linearity.

B. Signal Variance

The shot noise signal variance as a function of the mean signal within the linear photo response range of the CCD is shown in Fig. 7 for the three illumination wavelengths. The dependences are clearly non-linear, similar to the results in [3][4], and deviate from the straight line by 20% to 28%. The measured signal non-linearity is much too small to be a factor in the observed non-linearity in the variance.

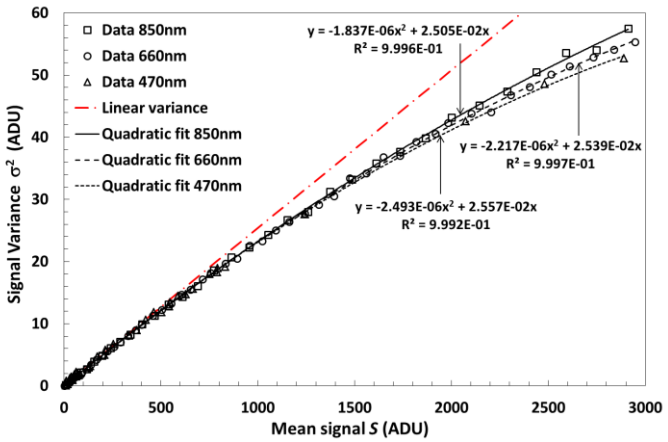

Fig. 7. Signal variance as a function of the mean signal for CCD204, fitted with the quadratic function (3). The linear variance line is calculated using the conversion gain from the 660 nm data.

A fit to the quadratic function (3) was applied to the experimental data and achieved excellent agreement. The quadratic term ν is seen to decrease with increasing wavelength, in line with the considerations for the characteristics of the charge sharing process.

Despite this excellent agreement, the MC model explains

the experimentally measured sub-Poisson variance only *qualitatively* because the charge sharing parameter α is not derived from device parameters and operating conditions. Also, the experimental data does not allow one to distinguish between the LN and RN charge sharing models because both produce quadratic mean-variance dependence. Further data will be required to establish the exact dependence of ν on different device parameters like thickness of the depleted region and the electric field.

C. Conversion Gain

The linear term in (3) can be used to calculate the system conversion gain in terms of e-/ADU. Because the equation (3) is much better fit to the experimental data than a straight line, the obtained gain is expected to be closer to the actual system gain.

At 660 nm the calculated conversion gain $K = 1/\gamma$ using (3) is $K = 39.4$ e-/ADU. The quadratic dependence of the PTC would cause the conversion gain to be overestimated if a linear fit to all data points is applied. A linear fit to the 660 nm data in Fig. 7 would produce gain K_{all} = 48.5 e-/ADU, a difference of 23% over the value derived from (3). To avoid this large error the usual practice has been to use only the data at short integration times, where the PTC is almost linear. From the first 10 seconds integration time the conversion gain is obtained as K_{10s} = 42.5 e-/ADU, still about 8% higher than the quadratic fit.

The proposed equation (3) uses all the available PTC points up to nearly full well and does not require that only a sufficiently linear section at low signals is selected. The requirement that the PTC data corresponds to linear photo response, as is the case in Fig. 2, is valid for all methods regardless of the number of points or formula used.

IV. Conclusion

This work presents a model describing the non-linearity of the PTC observed in many back-side illuminated, deep depleted CCDs. The effect is modeled as signal-dependent charge sharing during charge collection, leading to sub-Poison signal variance. This mechanism is distinct from the Fano factor as it occurs during charge collection and not charge generation, and is a non-linear function of the signal. The model predicts quadratic dependence of the shot noise dominated signal variance on the mean signal, and achieves excellent agreement with experimental data. The derived quadratic fit to the mean-variance data can be used for more robust calculation of the conversion gain in image sensors.

V. Acknowledgment

The author would like to thank Andrew Clarke and Neil Murray for providing the experimental data, and to Andrew Holland, Dan Weatherill and Paul Garthwaite for the useful and stimulating discussions.

References

[1] J. Janesick, "Photon Transfer Curve", in *Photon Transfer λ→DN*, Bellingham, WA: SPIE Press, 2007, pp. 49-71.

[2] B. Pain and B. Hancock, "Accurate estimation of conversion gain and quantum efficiency in CMOS imagers", *Proc. SPIE*, vol. 5017, pp. 94-103, 2003.

[3] M. Downing, D. Baade, P. Sinclaire, S. Deiries and F. Christen, "CCD riddle: a) signal vs time: linear; b) signal vs variance: non-linear", *Proc. SPIE*, vol. 6276, 627609, 2006.

[4] M. Downing, D. Baade, S. Deiries and P. Jorden. (2009, Oct.) Bulk Silicon CCDs, Point Spread Function and Photon Transfer Curves: CCD Testing Activities at ESO, Presented at Detectors for Astronomy Workshop, October 12 - 16, 2009, Garching. [Online]. Available: http://www.eso.org/sci/meetings/2009/dfa2009/program.html.

[5] R.K. Reich, "Sub-Poisson Statistics Observed in an Electronically Shuttered and Back-Illuminated CCD Pixel", *IEEE Trans. Electron Dev.*, vol. ED-44, no. 1, pp. 69-73, Jan. 1997.

[6] J.A. Fairfield, D.E. Groom, S.J. Bailey, C.J. Bebek, S.E. Holland, A. Karcher, W.F. Koble, W. Lorenzon and N.A. Roe, "Reduced Charge Diffusion in Thick, Fully Depleted CCDs With Enhanced Red Sensitivity", *IEEE Trans. Nucl. Sci*., vol. 53, no. 6, pp. 69-73, Dec. 2006, pp. 3877- 3881.

[7] J. Janesick, "Charge Collection", in *Scientific Charge Coupled Devices*, Bellingham, WA: SPIE Press, 2001, pp. 273-278.